Field Solution, Polarization, and Eigenmodes of Shielded Microstrip Transmission Line

ESSAM E. HASSAN

Abstract—**Application of the reciprocity theorem leads to a variational expression for the propagation constant of the fields inside shielded microstrip-like transmission lines. The resulting equation involves both the propagation constant and the tangential fields at the air–dielectric interface. Using the Rayleigh–Ritz optimization technique, both the propagation constant and the fields are completely determined.**

The calculated results of the propagation constant compare well with other available data. Moreover, the field solution obtained is presented in the form of a polarization ratio relating the axial to the transverse electric field. Results cover both low and high frequencies, and the technique proves valid at both frequency ranges. The method may be extended to other configurations of planar striplines by proper adjustment of the integration limits.

I. Introduction

THE problem of solving for the dispersion characteristics of shielded microstrip line has been tackled by many authors, either using the quasi-TEM theory [1]–[4] or through more rigorous analytical techniques [5]–[8]. Results for higher order modes have been reported by several authors [8]–[11]. Most of the techniques used involve some large set of equations to be numerically solved. In all data so far published in the literature, nothing or very little has been said about the form of the field inside the structure. This field is neither a purely TE nor a purely TM mode, rather it is a hybrid mode and cannot be directly obtained from a single scalar potential. A thorough understanding of this field configuration is an important factor in both the efficiency and the proper operation of many devices employing the microstrip line. This paper presents a powerful method to obtain both the field distribution and the propagation modes supported by this structure. The method is based on the application of the reciprocity theorem in the two domains comprising the shielded line. This leads to a variational expression for the propagation constant in the form of an integral equation linking the fields at the air–dielectric interface. With a proper field expansion and the Rayleigh–Ritz optimization technique, the relative amplitudes of the field components are determined, and the integral equation lends itself to a simple transcendental equation similar in nature to those of the LSE and LSM modes in the dielectric-loaded waveguide. A similar technique has been employed earlier by Rumsey [12] and by Harrington [13] in their treatment of radiation from an axially slotted waveguide. Numerical results using this method are presented for several cases, which compare well with the published data [9], [10], [17]. The method, in addition, points out the close relationship between the higher order modes and their counterparts of the LSE and LSM modes of the dielectric-loaded waveguide. Finally, the technique can easily be extended to handle the coplanar stripline [14], [15] and the various forms of microstrip transmission lines.

Manuscript received May 30, 1985; revised February 24, 1986. This work was supported by the University of Petroleum and Minerals, Dhahran, Saudi Arabia.

The author is with the Department of Electrical Engineering, University of Petroleum and Minerals, Dhahran 31261, Saudi Arabia.

IEEE Log Number 8608832.

II. Formulation of the Problem

A. Field Components

Fig. 1 shows a microstrip-like transmission line with two lossless dielectric layers. Region I has a relative dielectric constant ϵ_r and Region II is free space. The metal strip is of width $2t$ and assumed to be perfectly conducting with negligible thickness. The metallic shield enclosure is assumed of infinite conductivity and of width $2L$ and height h, and the dielectric layer of Region I is of height d. Although the technique presented here is quite general and could be easily applied to any number of inner conductors once the proper integral limits are considered, the analysis will be restricted to the case of a single conductor symmetrically placed inside the enclosure as shown in Fig. 1. In this inhomogeneous structure, the fields cannot be assumed to be purely TE or TM modes, rather a superposition of both TE and TM is unavoidable. Let the TE modes be derived from a scalar potential Ψ_i^e and the TM modes be derived from a scalar potential Ψ_i^h ($i=1$ or 2 depending on the region). It is necessary to point out here that because of the symmetry of the structure, two orthogonal sets of modes exist. The first has a symmetric E_z and an antisymmetric H_z (this mode is known as E_z even–H_z odd), and the other has an antisymmetric E_z and a symmetric H_z (known as E_z odd–H_z even). The TEM-like mode is the lowest order E_z even–H_z odd mode [17]. The analysis will be carried out for the E_z even–H_z odd modes, and the necessary modification for the solution of the other mode will be given whenever appropriate. Now let the scalar potentials for the E_z even–H_z odd modes be given by

$$\Psi_1^e = \sum_{n=1}^{\infty} A_n^e \sinh \alpha_n^{(1)} x \sin \gamma_n y \vec{a}_x \qquad \text{for Region I}$$

$$\Psi_1^h = \sum_{n=1}^{\infty} A_n^h \cosh \alpha_n^{(1)} x \cos \gamma_n y \vec{a}_x$$

0018-9480/86/0800-0845$01.00 ©1986 IEEE

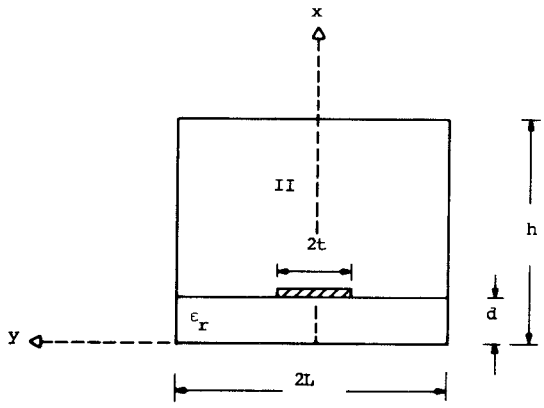

Fig. 1. Microstrip configuration.

and

$$\Psi_2^e = \sum_{n=1}^{\infty} B_n^e \sinh\alpha_n^{(2)}(h-x)\sin\gamma_n y\vec{a}_x$$

for Region II

$$\Psi_2^h = \sum_{n=1}^{\infty} B_n^h \cosh\alpha_n^{(2)}(h-x)\cos\gamma_n y\vec{a}_x \tag{1}$$

where the factor $\exp j(\omega t-\beta z)$ is understood and

$$\gamma_n = (2n-1)\Pi/2L, \qquad n=1,2,3,\cdots$$

$$\alpha_n^{(1)} = \sqrt{\gamma_n^2+\beta^2-K_1^2}$$

$$\alpha_n^{(2)} = \sqrt{\gamma_n^2+\beta^2-K_0^2}$$

A_n^h, A_n^e, B_n^h, and B_n^e are unknown coefficients

$$K_0^2 = \omega^2\mu_0\epsilon_0 \qquad K_1^2 = \epsilon_r K_0^2.$$

ϵ_0 and μ_0 are the permittivity and the magnetic permeability of free space, and ϵ_r is the relative permittivity of medium I. With $\omega = 2\Pi f$ the operating frequency (rad/s), β is the desired propagation constant. For the E_z odd–H_z even modes the term $\sin\gamma_n y$ replaces $\cos\gamma_n y$, and vice versa. Also, $\gamma_n = n\pi/L$, and the summation should start from 0 to ∞.

The hybrid field components are derived from the above scalar potential in a way similar to that presented in [8]. Applying the appropriate boundary conditions of the tangential electric and magnetic fields along the plane $x=d$ and using the orthogonality of sinusoidal functions, the coefficients A_n^h, A_n^e, B_n^h, and B_n^e may all be obtained in terms of the integrals $I_y(n)$ and $I_z(n)$ defined as [8]

$$I_y(n) = \int_t^L E_y\Big|_{x=d}\sin\gamma_n y\,dy$$

$$I_z(n) = \int_t^L E_z\Big|_{x=d}\cos\gamma_n y\,dy. \tag{2}$$

By substituting this set of coefficients in (1), all field components in either region are readily obtained in terms of the values of E_y and E_z along the plane $x=d$.

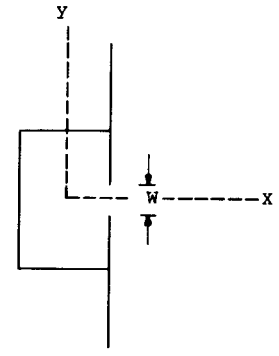

Fig. 2. Cross section of slotted waveguide.

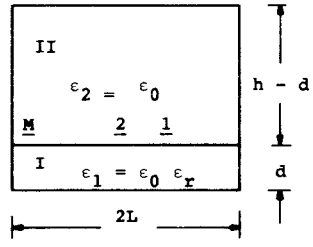

Fig. 3. Microstrip transmission line with M metal strips.

B. Variational Expression

Rumsey, in his treatment of the leaky wave slotted waveguide [12], has shown that a stationary expression for the propagation constant β of the cross section shown in Fig. 2 is

$$\phi = \int_{-W/2}^{W/2}\left[E_y\left({}^iH_z - {}^eH_z\right) + E_z\left({}^iH_y - {}^eH_y\right)\right]dy = 0 \tag{3}$$

where E_y and E_z are the components of the assumed electric field in the slot and ${}^iH$ and ${}^eH$ are the internal and the external magnetic fields which fit the assumed E_y and E_z. Using the same approach, a similar expression could be applied to the configuration of Fig. 1. Further, the integration could be taken along as many slots as there are in the interface between the two regions. Thus, for the configuration of Fig. 3, (3) becomes

$$\sum_{m=1}^{M}\int\left[E_{ym}\left({}^iH_{zm} - {}^eH_{zm}\right) + E_{zm}\left({}^iH_{ym} - {}^eH_{ym}\right)\right]dy = 0 \tag{4}$$

where the subscript m refers to the mth slot of a total of M slots. For the configuration of Fig. 1, using the field components as obtained from the scalar potentials (1) where the set of constants A_n^h, A_n^e, B_n^h, and B_n^e are all in terms of $I_y(n)$ and $I_z(n)$ and substituting in (3), one gets, after some manipulation, an expression of the form

$$\phi(n) = \sum_{n=1}^{\infty} S_n I_y^2(n) + \sum_{n=1}^{\infty} V_n I_y(n) I_z(n) + \sum_{n=1}^{\infty} U_n I_z^2(n) = 0 \tag{5}$$

where

$$S_n = -\frac{2j}{\omega\mu_0 L}\left[(\beta^2 - K_1^2)G_1(n) + (\beta^2 - K_0^2)G_2(n)\right]$$

$$V_n = -\frac{4\beta\gamma_n}{\omega\mu_0 L}\left[G_1(n) + G_2(n)\right]$$

$$U_n = \frac{2j}{\omega\mu_0 L}\left[(K_1^2 - \gamma_n^2)G_1(n) + (K_0^2 - \gamma_n^2)G_2(n)\right]$$

with

$$G_1(n) = \coth\alpha_n^{(1)} d/\alpha_n^{(1)}$$

$$G_2(n) = \coth\alpha_n^{(2)}(h-d)/\alpha_n^{(2)}.$$

Equation (5) has three unknowns, the propagation constant β and the slot electric fields E_y and E_z. As mentioned previously, (5) is a stationary expression for β, and reasonable assumed values for E_y and E_z when substituted in it will yield a very close approximation to the true value of β. The electric field components at $x = d$ are to be expanded in a set of orthogonal functions with unknown coefficients (a_p's and b_q's) in the form

$$E_y|_{x=d} = \sum_{p=1}^{\infty} a_p \sin\frac{(2p-1)\pi}{2(L-t)}(y-t)$$

$$E_z|_{x=d} = \sum_{q=1}^{\infty} b_q \cos\frac{(2q-1)\pi}{2(L-t)}(y-t) \qquad (6)$$

with a_1 normalized to unity.

Substituting (6) in (5), one gets the stationary expression of β in terms of the coefficients a_p and b_q. Now, since the assumed field expansion is a complete set, the Rayleigh–Ritz optimization procedure could be applied to the resulting equation by successively differentiating $\phi(n)$ with respect to a_p's and b_q's and setting the result to zero, i.e.,

$$\frac{d\phi(n)}{da_p} = 0, \qquad p = 2,3,4,\cdots \qquad (7a)$$

$$\frac{d\phi(n)}{db_q} = 0, \qquad q = 1,2,3,\cdots. \qquad (7b)$$

This optimization technique must, in principle, obtain the true values of the field as the number of terms in the expansion (6) approaches infinity. The successive differentiations as given by (7a) and (7b) when truncated at P and Q, respectively, will result in a set of $(P+Q-1)$ equations in the unknown coefficients $a_2, a_3, \cdots, a_p$ and $b_1, b_2, \cdots, b_Q$ along with β. This set, along with (5), may be solved as shown later to determine both β and the unknown coefficients. Once these coefficients are known, all field components are readily obtained. Detailed discussion of the solution is presented in Section III of this paper.

It is interesting at this stage to examine the very simple case of $P = Q = 1$. In such case, with $a_1 = 1$ one gets

$$b_1 = -\left[\sum_{n=1}^{\infty} V_n I_y(n) I_z(n)\right] \Big/ \left[2\sum_{n=1}^{\infty} U_n I_z^2(n)\right]. \qquad (8)$$

Substituting back in (6) and using the result in (5), the latter will take the form

$$\sum_{n=1}^{\infty}\left[(K_1^2 - \beta^2)G_1(n) + (K_0^2 - \beta^2)G_2(n)\right] I_y^2(n) - \left\{\beta^2\left[\sum_{n=1}^{\infty}\gamma_n(G_1(n)+G_2(n))I_y(n)I_z(n)\right]^2 \Big/ \sum_{n=1}^{\infty}\left[(K_1^2-\gamma_n^2)G_1(n) + (K_0^2-\gamma_n^2)G_2(n)\right] I_z^2(n)\right\} = 0. \qquad (9)$$

If a further simplification is made and we consider only the $n = 1$ term of (9), the resulting expression will satisfy the characteristic equations for the LSE and the LSM of the corresponding partially dielectric-filled waveguide, namely [16],

$$\alpha_1^{(1)}\cot\alpha_1^{(1)} d = -\alpha_1^{(2)}\cot\alpha_1^{(2)}(h-d) \qquad \text{for LSE}$$

and

$$\epsilon_r\frac{\cot\alpha_1^{(1)} d}{\alpha_1^{(1)}} = -\frac{\cot\alpha_1^{(2)}(h-d)}{\alpha_1^{(2)}} \qquad \text{for LSM.} \qquad (10)$$

This establishes analytically the closeness of the solution of the propagation mode for the LSE and LSM of the dielectric loaded waveguide and the corresponding shielded microstrip line, a fact that has been observed numerically [9].

The analysis for the E odd–H even modes follows the same steps and will yield an expression similar to (9). However, the sine and cosine terms of the assumed slot field, (6), should be interchanged. Further, in (1) the summation over n starts at $n = 0$, and the $n = 0$ term should be halved.

III. Solution of the Problem

As explained earlier, the solution is based on combining (5) along with (7). This results in the following set of equations:

$$\sum_{n=1}^{N} 2S_n f_i(n) \sum_{p=2}^{P} a_p f_p(n) + \sum_{n}^{N} V_n f_i(n) \sum_{q=1}^{Q} b_q g_q(n) = -\sum_{n=1}^{N} 2S_n f_i(n) f_1(n), \qquad i = 2,3,\cdots,P$$

and

$$\sum_{n=1}^{N} V_n g_j(n) \sum_{p=2}^{P} a_p f_p(n) + \sum_{n=1}^{N} 2U_n g_j(n) \sum_{q=1}^{Q} b_q g_q(n) = -\sum_{n=1}^{N} V_n g_j(n) f_1(n), \qquad j = 1,2,3,\cdots,Q \qquad (11)$$

where

$$f_p(n) = \int_t^L \left\{\sin\left[(2p-1)\pi\frac{(y-t)}{2(L-t)}\right]\cdot\sin\gamma_n y\right\} dy$$

and

$$g_q(n) = \int_t^L \left\{ \cos\left[(2q-1)\pi \frac{(y-t)}{2(L-t)} \right] \cdot \cos \gamma_n y \right\} dy.$$

These are $(P-1+Q)$ simultaneous linear equations in the unknowns $a_2, a_3, \cdots, a_p, b_1, b_2, \cdots, b_Q$. Notice that the propagation constant β is still unknown and is part of the coefficients of the set (11). To complete the solution, (5) is added to the set (11). The solution for β is sought first, and once it is known the field coefficients are readily obtained. The technique adopted is straightforward. We assume a value for β which is chosen close to the true value. (This is chosen in the vicinity of the value of the propagation constant for the corresponding mode of a similar dielectric loaded waveguide, for the non-TEM mode, and is chosen to be $\sqrt{(1+\epsilon_r)/2}\,K_0$ for the TEM mode.) The coefficients a_p and b_q are then obtained from (11) for the assumed value of β, and the result is substituted in (5), which must be zero for the true value of β. The procedure is iterated until the zero is captured. The value of β is then obtained, and the coefficients a_p and b_q, hence the field solutions, are readily available. In the following section, some results are presented and discussed.

IV. Results and Discussion

A. TEM Mode

Figs. 4 and 5 represent the normalized propagation constant β/K_0 as a function of frequency, compared with results published in [8], [9], and [18]. The results of this paper are presented for frequencies up to 50 MHz and, if desired, could be easily extended to higher frequencies. The results are shown to be almost identical with those of the nonuniform discretization of integral equation [9] and very close to the results of [10] in all frequency spectrums tested up to 50 MHz. This verifies the accuracy of the technique. Such good agreement with [9], [10] seems to have its importance at the high frequency region where discrepancy is noticed between our work and other methods presented here [8], [18] or presented in [9]. The accuracy of the empirical formulas [19], [20] seems to be inaccurate by a considerable margin at high frequencies [9].

Convergence towards the true value of β could be obtained in a relatively small number of expansion terms. When the expansion of (6) is truncated at $p=q=10$, a 3–4 percent discrepancy of the true value of β is noticed. Such convergence with a low number of terms and subsequently low computational time is indeed expected to be due to the stationary nature of the expression. If higher accuracy is desired, a higher number of expansion terms could be used. In the results presented here, an initial iteration at $p=q=8$ is executed starting at a value of $\beta = \sqrt{(1+\epsilon_r)/2} \cdot K_0$. When the root is captured, it is used as a starting iteration for a second stage at $p=q=20$ to 22. In all cases examined, such a number of terms would result in a stable value of β. Table I presents an example of such a result for the specific case indicated. The number of expansion terms used is comparable with that of the integral equation method of [9]. Examination of the results shows that the value of β/K_0 seems to tend to a constant value as the frequency increases. Investigating several results shows that this limiting value approaches $\sqrt{\epsilon_r}$. For

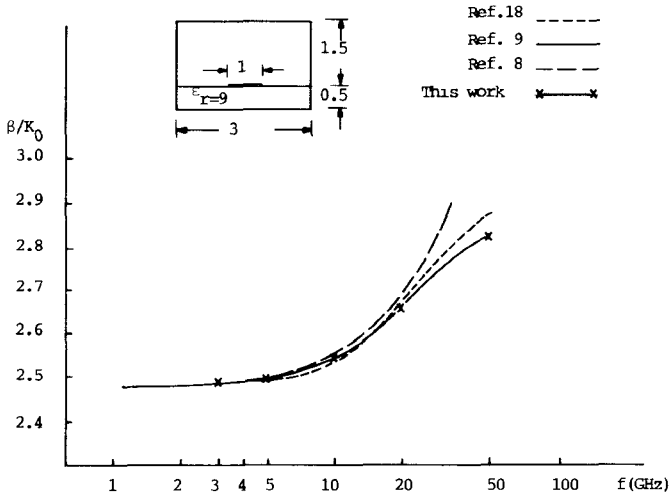

Fig. 4. Variation of β/K_0 with frequency compared with other methods. Units are in millimeters.

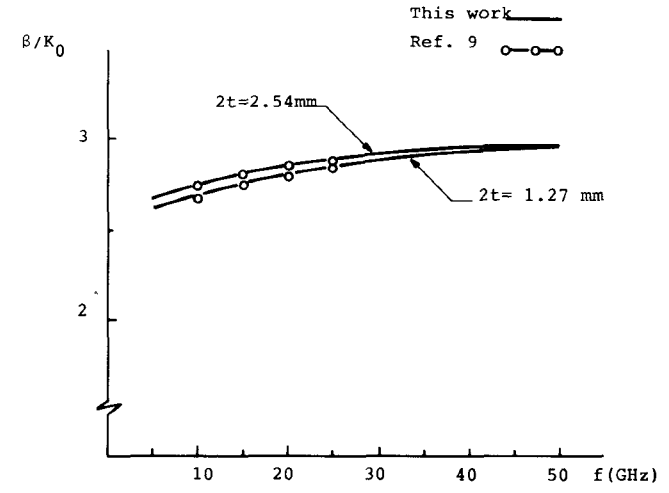

Fig. 5. Variation of β/K_0 with frequency. $\epsilon_r = 8.875$, $2L = 12.7$ mm, $h = 12.7$ mm, $d = 1.27$ mm.

TABLE I
Convergence of the Root β/K_0 Against the Number of Expansion Terms

P	Q	β/K_0
3	3	3.1535
6	6	2.9405
10	10	2.8593
20	20	2.7968
22	22	2.7906
23	23	2.7885

$f = 15$ GHz, $2t = 1.905$ mm, $2L = 12.7$ mm, $\epsilon = 8.875$, $d = 1.27$ mm, $h = 12.7$ mm.

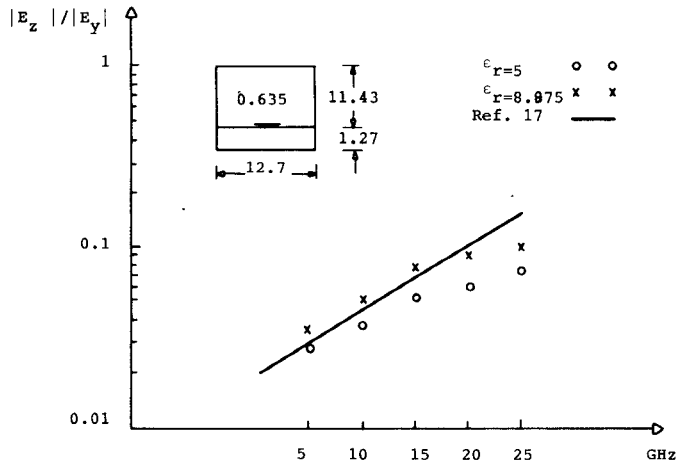

Fig. 6. Polarization versus frequency compared with data published in [17]. Units are in millimeters.

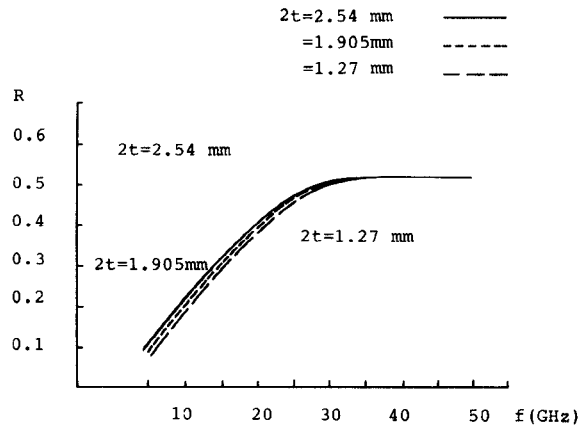

Fig. 7. Variation of polarization ratio R with frequency. Parameters are those of Fig. 5.

example, the result shown in Fig. 5 for $\epsilon_r = 8.875$ tends to about 2.96 while $\sqrt{\epsilon_r}$ is 2.979. Other results available to the author (not shown here) showed that for $\epsilon_r = 5$ and 12 the limiting values are around 2.18 and 3.45, respectively, which are very close to $\sqrt{5} = 2.23$ and $\sqrt{12} = 3.46$. It is also found that in such case, the higher the value of ϵ_r, the closer the ratio (limiting value of $[\beta/K_0]/\sqrt{\epsilon_r}$) is to unity. This result indicates that the field in the very-high-frequency case would possibly concentrate in the dielectric region acquiring its mode of propagation.

Turning our attention now to the field polarization, Figs. 6 and 7 present some examples of the results obtained. These results are obtained by evaluating the coefficients a_p and b_q of the expansion (6) as indicated in the theory. Numerical evaluation shows that a large number of terms of the expansion (6) are needed to obtain stabilized values for the first few terms. Fig. 8 shows the convergence of the first term of each of the a_p's and b_q's. It is clear that they are slowly approaching a limit as the number of terms increases. In all calculations of the polarization ratio R of Fig. 7 (defined as $|E_z|/\sqrt{|E_x^2|+|E_y^2|}$) or polarization P of Fig. 6, up to 22 terms of each expansion are considered to approach as accurately as possible the true value of the field. It is found that inclusion of higher number of terms does not alter the value of R appreciably. Fig. 6 shows a plot of the polarization $|E_z|/|E_y|$ versus frequency for two different values of ϵ_r as compared with the only data available to the author. This comparison is the reason to consider $|E_Z|/|E_Y|$ and not the axial-to-total field ratio (i.e., $|E_z|/\sqrt{|E_x^2|+|E_y^2|}$ as considered in Fig. 7). Results show that the axial component of the electric field E_z is negligibly small at low frequencies where the field approaches true TEM. In fact, the quasi-TEM theory as shown in [17] is highly accurate at this region. At higher frequencies, however, the value of the axial field component E_z increases and the field deviates from the TEM-like mode. Fig. 6 shows this general trend for two different values of dielectric constant ϵ_r compared with data published in [17]. The agreement is quite remarkable. It is shown that the polarization ratio decreases as ϵ_r decreases, which is expected since as ϵ_r approaches unity one should expect a true TEM mode inside the structure. In Fig. 7, the polarization ratio R versus frequency is presented for several different strip widths. The same general trend of very low R at low frequency is observed. Also, it seems that the polarization ratio tends towards a limit at wavelength comparable to the structure dimensions. Further work is under way to investigate analytically such limit. It is clear that the ratio R is insensitive to the strip width, but is primarily a function of frequency and dielectric constant as evident from Figs. 6 and 7.

B. Higher Order Modes

Higher order modes were also investigated with respect to both their propagation constant and polarization ratio. Figs. 9 and 10 give the value of β/K_0 compared with data published in the literature. Results are almost typical of those of [9]. However, this technique has the advantage of being highly convergent. Table II shows a sample of the results available where a total of only five terms was sufficient to obtain a value for β/K_0 with an error less than 0.4 percent. This was noticed in all results examined for the first as well as the higher-order modes. The similarity of the $f-\beta$ characteristics of these curves and the LSE or LSM is evident and is discussed elsewhere [8], [9]. The study of the polarization factor (Fig. 11) reveals the same general characteristics observed in the TEM-like modes. The value of R is low at low frequencies but, compared to the TEM mode, it increases appreciably as the frequency increases. They seem to tend to a limit. However, extra work is needed to investigate such limiting value. Further, the value of R decreases—as expected—with the lower value of ϵ_r. The convergence of the coefficients of expansion (6) is found to be much faster here than in the TEM case. An example of this convergence is given in Table III. Such difference in convergence may be attributed to the difference in behavior between the TEM and the higher order modes. While the expansion (6) is most suited for the higher order modes, it might be more appropriate (for fast convergence) to assume an expansion for the TEM which

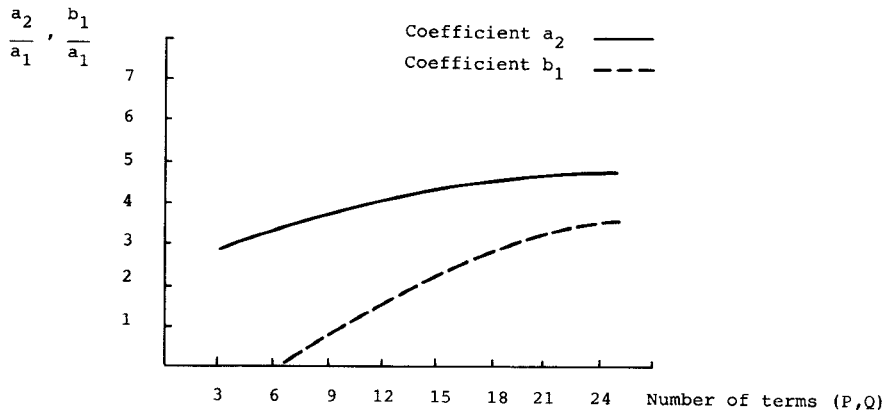

Fig. 8. Convergence of a_2 and b_1. Parameters are $\epsilon_r = 8.875$, $f = 15$ GHz, $2t = 1.905$, $2L = 12.7$, $h = 12.7$, $d = 1.27$. All dimensions are in millimeters.

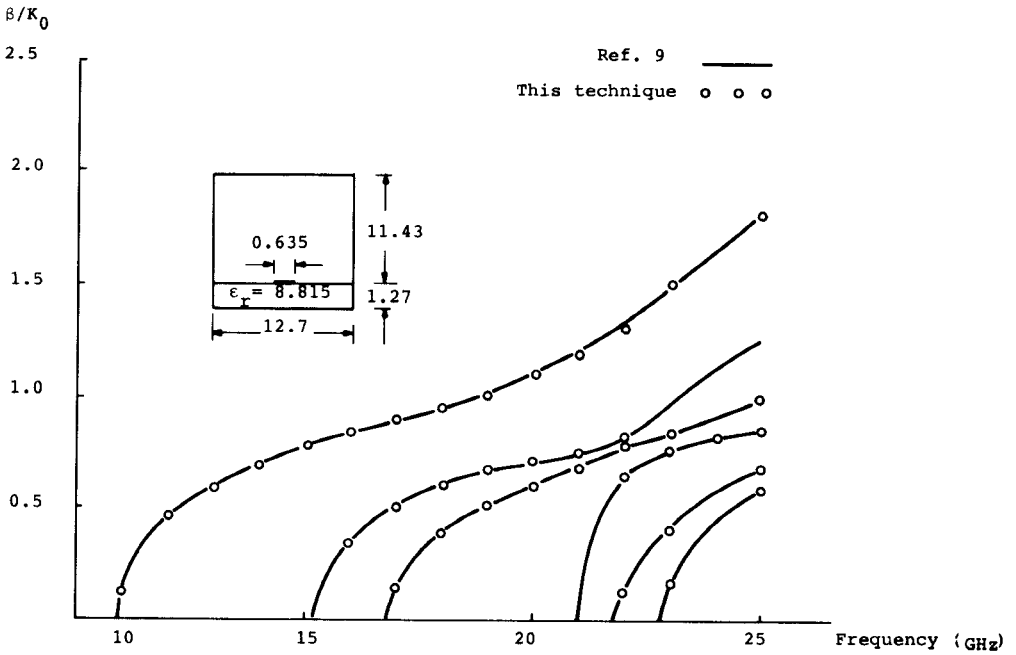

Fig. 9. The $f-\beta$ characteristics of microstrip transmission line with strip width 0.635 mm for E even–H odd modes compared with other published data (dimensions are in millimeters).

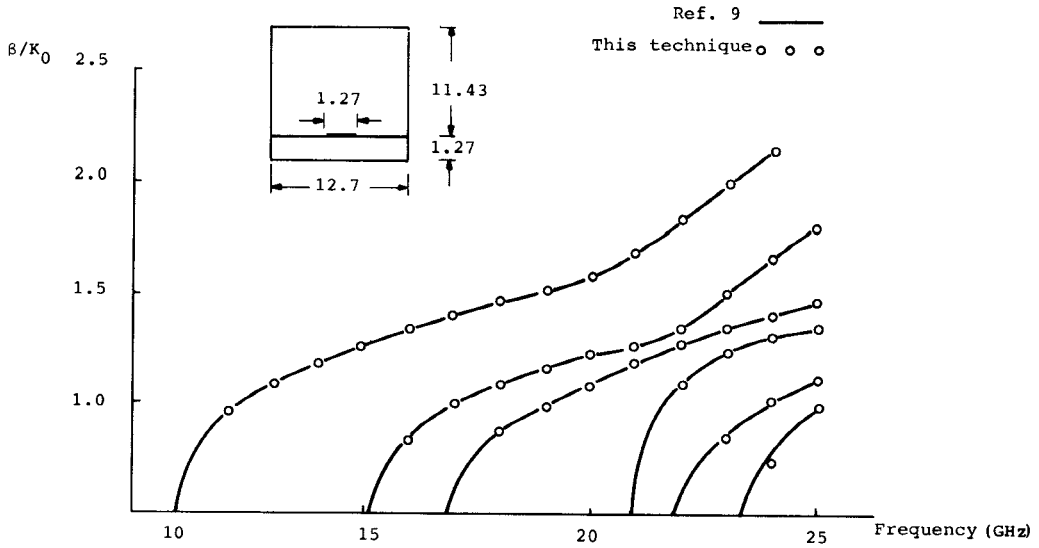

Fig. 10. The $f-\beta$ characteristics of microstrip transmission line with strip width 1.27 mm for E even–H odd modes compared with other published data (dimensions are in millimeters).

TABLE II
CONVERGENCE OF THE PROPAGATION CONSTANT.

	f = 15 GHz			f = 25 GHz			
No. of terms M	3, 3	6, 6	9, 9	3, 3	6, 6	9, 9	12, 12
Root β/K_0	0.780	0. 784	0.785	1.754	1.7592	1.7580	1.7576

Parameters are those of Fig. 9.

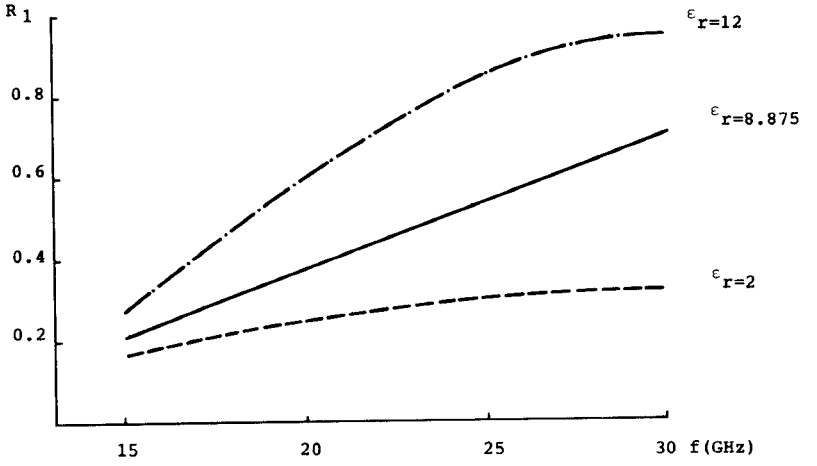

Fig. 11. Polarization R of the first mode for different values of ϵ_r. Parameters are those of Fig. 9.

TABLE III
EXAMPLE OF CONVERGENCE OF THE COEFFICIENTS OF EXPANSION (8)

Number of terms M	a_2	a_3	b_1	b_2	b_3
(3, 3)	-0.627	0.124	-2.5	1.20	0.2
(6, 6)	-0.66	0.088	-2.57	1.27	0.21
(8, 8)	-0.684	0.076	-2.61	1.30	0.22
(10,10)	-0.694	0.067	-2.61	1.317	0.224
(12,12)	-0.700	0.062	-2.61	1.320	0.227

For the parameters of Fig. 9 ($f = 25$ GHz).

takes into account the similarity between the TEM and the corresponding static field for the same configuration.

Polarization for higher order modes is also investigated. The general behavior is the same as for the TEM mode, and they carry no new information to present.

V. CONCLUSION

This paper presents a variational technique to solve for the dispersion characteristics as well as the field configuration inside the shielded microstrip transmission line. The technique allows for rapid convergence of the propagation constant due to the variational nature of the expression, and the results are very close to results published previously. Further, the field solution is obtained and compares well with the only data available to the author. Higher order modes were also investigated, and the similarity between such modes and those of the LSE and LSM was shown both analytically and numerically.

ACKNOWLEDGMENT

The research of this paper was carried out in the Electrical Engineering Department, University of Petroleum and Minerals, Dhahran, Saudi Arabia.

REFERENCES

[1] H. A. Wheeler, "Transmission-line properties of parallel strips separated by a dielectric sheet," *IEEE Trans. Microwave Theory Tech.*, vol. MTT-13, pp. 172–185, Mar. 1965.
[2] T. G. Bryant and J. A. Weiss, "Parameters of microstrip transmission lines and of coupled pairs of microstrip lines," *IEEE Trans. Microwave Theory Tech.*, vol. MTT-16, pp. 1021–1027, Dec. 1968.
[3] M. K. Krage and G. I. Haddad, "Characteristics of coupled microstrip transmission lines—II: Evaluation of coupled line parameters," *IEEE Trans. Microwave Theory Tech.*, vol. MTT-18, pp. 222–228, Apr. 1970.
[4] P. Silvester, "TEM wave properties of microstrip transmission lines," *Proc. Inst. Elec. Eng.*, vol. 115, pp. 43–48, Jan. 1968.
[5] P. Daly, "Hybrid-mode analysis of microstrip by finite element methods," *IEEE Trans. Microwave Theory Tech.*, vol. MTT-19, pp. 19–25, Jan. 1971.
[6] E. J. Denlinger, "A frequency dependent solution for microstrip transmission lines," *IEEE Trans. Microwave Theory Tech.*, vol. MTT-19, pp. 30–39, Jan. 1971.
[7] G. I. Zysman and D. Varon, "Wave propagation in microstrip transmission lines," in *1969 Int. Microwave Symp. Dig.* (Dallas, TX), 1969, pp. 3–9.
[8] R. Mittra and T. Itoh, "A new technique for the analysis of the dispersion characteristics of microstrip lines," *IEEE Trans. Microwave Theory Tech.*, vol. MTT-19, pp. 47–56, Jan. 1971.
[9] E. Yamashita and K. Atsuki, "Analysis of microstrip-like transmission lines by nonuniform discretization of integral equations,"

IEEE Trans. Microwave Theory Tech., vol. MTT-24, pp. 195–200, Apr. 1976.
[10] G. Kowalski and R. Pregla, "Dispersion characteristics of shielded microstrips with finite thickness," *Arch. Elek. Übertragung.*, vol. 107, pp. 163–170, Apr. 1971.
[11] J. S. Hornsby and A. Gopinath, "Numerical analysis of a dielectric loaded waveguide with a microstrip line—Finite difference method," *IEEE Trans. Microwave Theory Tech.*, vol. MTT-17, pp. 684–690, Sept. 1969.
[12] V. Rumsey, "Travelling wave slot antennas," *J. Appl. Phys.*, vol. 24, pp. 1358–1365, Nov. 1953.
[13] R. F. Harrington, "Propagation along a slotted cylinder," *J. Appl. Phys.*, vol. 24, pp. 1366–1371, Nov. 1953.
[14] C. P. Wen, "Coplanar waveguide: A surface strip transmission line suitable for non-reciprocal gyromagnetic device applications," *IEEE Trans. Microwave Theory Tech.*, vol. MTT-17, pp. 1087–1090, Dec. 1969.
[15] S. B. Cohn, "Slot line on a dielectric substrate," *IEEE Trans. Microwave Theory Tech.*, vol. MTT-17, pp. 768–778, Oct. 1969.
[16] R. F. Harrington, *Time-Harmonic Electromagnetic Fields*. New York: McGraw-Hill, 1961.
[17] L. Young and H. Sobol, Eds., *Advances in Microwaves*, vol. 8. New York: Academic Press, 1974.
[18] W. J. Getsinger, "Microstrip dispersion model," *IEEE Trans. Microwave Theory Tech.*, vol. MTT-21, pp. 34–39, Jan. 1973.
[19] M. V. Schneider, "Microstrip dispersion," *Proc. IEEE*, vol. 60, pp. 144–146, Jan. 1972.
[20] H. J. Carlin, "A simplified circuit model for microstrip," *IEEE Trans. Microwave Theory Tech.*, vol. MTT-21, pp. 589–591, Sept. 1973.

✠

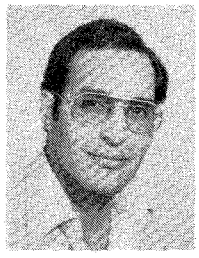

Essam E. Hassan was born in Alexandria, Egypt in 1947. He received the B.Sc. degree in electrical engineering (with honors) from Alexandria University in 1970, and the M.Sc. and Ph.D. degrees in electrical engineering from the University of Manitoba, Winnipeg, Canada, in 1977 and 1978, respectively.

From 1977 to 1979, he was a Senior Research Engineer with Northern Telecom Canada in the digital switching division, where he was responsible for design and testing of digital networks. In 1979, he joined the Department of Electrical Engineering at the University of Petroleum and Minerals, Dhahran, Saudi Arabia, and since then he has been active in the fields of communication, microwave communication, and electromagnetics field theory.

Dr. Hassan is an author or coauthor of several technical papers in electromagnetics and in communication as well as one book in communication theory.